Ab Initio Configuration Interaction and Random Phase Approximation Calculations of the Excited Singlet and Triplet States of Adenine and Guanine

James D. Petke,* Gerald M. Maggiora, and Ralph E. Christoffersen†

Contribution from Computational Chemistry, The Upjohn Company, 301 Henrietta Street, Kalamazoo, Michigan 49001. *Received October 30, 1989*

Abstract: The electronic absorption spectra of adenine and guanine have been calculated with ab initio multi-reference configuration interaction (MRCI) and random phase approximation (RPA) methods, using ground-state self-consistent field orbitals obtained with a double-ζ/polarization/diffuse Cartesian Gaussian basis set. Between 20 and 25 singlet-singlet transitions of varying intensity were found to contribute to the spectral region from 35 000 to 55 000 cm^{-1} of each molecule. Transition energy errors from both the MRCI and RPA studies were found on average to fall within a range of 12 000 to 15 000 cm^{-1}, and a linear scaling of calculated transition energies was used to produce a qualitative resolution of the absorption spectra. In adenine, the lowest absorption band at 38 500 cm^{-1} (band I) was found to arise from a group of five electronic transitions, two $\sigma \rightarrow \pi^*$ and three $\pi \rightarrow \pi^*$, but only one $\pi \rightarrow \pi^*$ transition was of high intensity. The calculated polarization of the intense transition did not agree with the experimental value obtained for adenine crystals. However, it was shown that the polarization of band I is likely to vary considerably with molecular environment, as well as being sensitive to the level of calculation. In guanine, the absorption maximum at 36 300 cm^{-1} (band I) was found to consist of two $\pi \rightarrow \pi^*$ transitions, while one $\sigma \rightarrow \pi^*$ and three $\pi \rightarrow \pi^*$ transitions were found to contribute to band II at 40 000 cm^{-1}. For each $\pi \rightarrow \pi^*$ transition, the excited state was found to contain a mixture of valence and Rydberg character. The polarizations of bands I and II could not be unequivocally determined, owing to the spectral congestion and sensitivity of the constituent excited states to the level of calculation. In the spectral region between 45 000 and 55 000 cm^{-1}, the calculations for both molecules revealed a large number of transitions of varying intensity. Although the MRCI and RPA calculations give different detailed descriptions of the spectrum, the general features of the broad-banded absorption of this spectral region are provided by both methods. MRCI calculations of triplet states showed that the lowest triplet state, T_1, in adenine lies approximately 24 930 cm^{-1} above the ground state, and that there are four valence triplet (π,π^*) states below the lowest excited singlet state. In guanine, valence states T_1 and T_2 were found at approximately 28 280 and 29 520 cm^{-1} above the ground state, while T_3 and T_4 were essentially isoenergetic with the lowest excited singlet state.

Introduction

Optical spectroscopic methods including UV absorption and emission, linear dichroism, and circular dichroism have proven to be important tools for monitoring nucleic acid structural changes as well as for probing interactions of DNA and RNA with proteins and small molecules.[1-3] As the application of spectroscopic techniques becomes more refined, however, an increased need for more detailed and reliable determination of structural information has emerged. One potential means of gaining insight into correlations among spectral and structural data is through theoretical studies of electronic spectra (e.g., circular dichroism) as a function of molecular conformation. For large systems such as polynucleotides, exciton-based methods[4,5] provide a tractable computational approach to the problem, but require a detailed knowledge of the electronic excited states, electron densities, and transition densities of the chromophoric units within the system. In this connection, the electronic absorption and emission spectra of the nucleic acids are due primarily to the spectral properties of the constituent purine and pyrimidine bases, which exhibit strong UV absorption in the frequency range 35 000–55 000 cm^{-1} (280–180 nm). It is therefore essential that a detailed understanding of this spectral region be obtained, in order that appropriate spectral-structural correlations and insights into biological processes be realized.

There have been numerous experimental and theoretical studies of the electronic excited states and spectra of the individual bases as well as of nucleosides and nucleotides; a comprehensive review of this material has been presented by Callis.[6] However, there remain many questions regarding the number and polarization of transitions, the location of $n \rightarrow \pi^*$ and other "hidden" transitions within the absorption bands, and the characteristics of low-lying triplet states. Recently, some of these questions have been addressed for cytosine by means of ab initio calculations of its excited electronic states. In particular, Matos and Roos[7] and Jensen et al.[8] have reported studies of the cytosine singlet–singlet absorption spectrum using extended basis MCSCF and RPA methods, respectively, and we are also preparing a report similar to the present study on cytosine and uracil (Petke et al., in preparation). From a computational viewpoint, the purine bases adenine and guanine place much greater demand on computer resources since they are considerably larger than pyrimidine bases, and thus to date all theoretical studies of the excited states of adenine and guanine have been performed using semiempirical approaches,[9-21] although

† Present address: SmithKline Beecham, P.O. Box 1539, King of Prussia, PA 19406.

(1) Hofrichter, J.; Eaton, W. A. *Annu. Rev. Biophys. Bioeng.* **1976**, *5*, 511–560.
(2) Steiner, R. F., Ed. *Excited States of Biopolymers*; Plenum: New York, 1983.
(3) Woody, R. W. *J. Polym. Sci. Macromol. Rev.* **1977**, *12*, 181–320.
(4) Tinoco, I., Jr. *Adv. Chem. Phys.* **1962**, *4*, 113–160.
(5) LaLonde, D. E.; Petke, J. D.; Maggiora, G. M. *J. Phys. Chem.* **1988**, *92*, 4746–4752.
(6) Callis, P. R. *Annu. Rev. Phys. Chem.* **1983**, *34*, 329–357.
(7) Matos, J. M. O.; Roos, B. O. *J. Am. Chem. Soc.* **1988**, *110*, 7664–7671.
(8) Jensen, H. J. A.; Koch, H.; Jorgensen, P. *Chem. Phys.* **1988**, *119*, 297–306.
(9) Berthod, H.; Giessner-Prettre, C.; Pullman, A. *Int. J. Quantum Chem.* **1967**, *1*, 123–137.
(10) Fugita, H.; Imamura, A.; Nagata, C. *Bull. Chem. Soc. Jpn.* **1968**, *41*, 2017–2026.
(11) Packer, J. C.; Avery, J. S.; Ladik, J.; Biczo, G. *Int. J. Quantum Chem.* **1969**, *3*, 79–92.
(12) Bailey, M. L. *Theor. Chim. Acta* **1970**, *16*, 309–315.
(13) Hug, W.; Tinoco, I. *J. Am. Chem. Soc.* **1973**, *95*, 2803–2813.
(14) Ito, H.; I'Haya, Y. J. *Bull. Chem. Soc. Jpn.* **1976**, *49*, 3466–3471.
(15) Srivastava, S. K.; Mishra, P. C. *Int. J. Quantum Chem.* **1979**, *16*, 1051–1068; **1980**, *18*, 827–840.
(16) Srivastava, S. K.; Mishra, P. C. *J. Mol. Struct.* **1980**, *65*, 199–213.
(17) Danilov, V. I.; Pechenaya, V. I.; Zheltovsky, N. V. *Int. J. Quantum Chem.* **1980**, *17*, 307–320.
(18) Kaito, A.; Hatano, M. *Bull. Chem. Soc. Jpn.* **1980**, *53*, 3064–3068.
(19) Grinberg, H.; Capparelli, A. L.; Spina, A.; Maranon, J.; Sorarrain, O. M. *J. Phys. Chem.* **1981**, *85*, 2751–2759.
(20) Shramko, O. V. *Theor. Eksp. Khim.* **1984**, *20*, 717–721.
(21) Callis, P. R. *Photochem. Photobiol.* **1986**, *44*, 315–332.

0002-7863/90/1512-5452$02.50/0

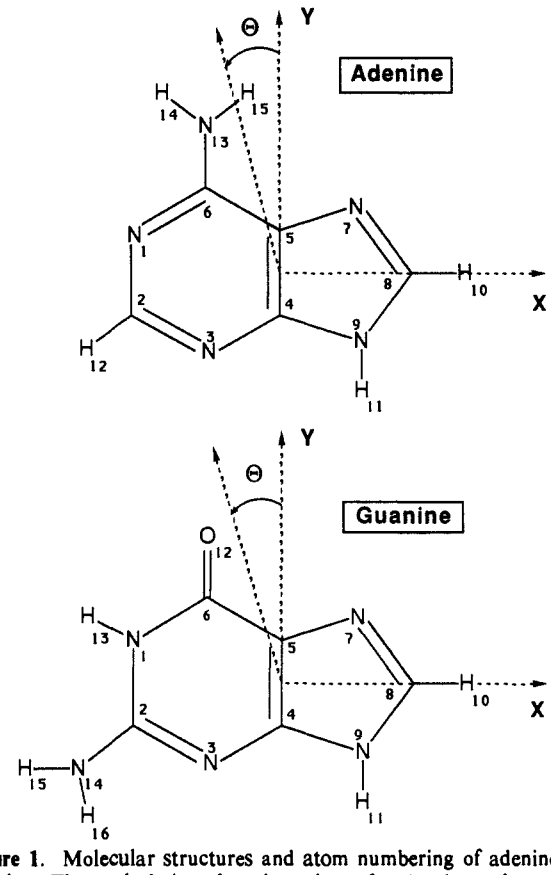

Figure 1. Molecular structures and atom numbering of adenine and guanine. The angle θ gives the orientations of molecular and transition dipole moment vectors relative to the y axis.

a number of ground-state ab initio calculations have been reported.[22-30] This report presents the results of the first ab initio quantum mechanical treatment of the ground and excited singlet and triplet states of adenine and guanine. Multi-reference configuration interaction (MRCI) calculations were performed on the ground and low-lying excited singlet and triplet states using ground-state self-consistent field (SCF) orbitals obtained with an extended basis set. In addition, random phase approximation (RPA) calculations were used to obtain singlet–singlet transition energies and intensities. The results are compared with available experimental and theoretical data, and the composition and resolution of the absorption spectra from 35 000 to 55 000 cm^{-1} is presented. As a result, it is believed that these studies provide both a rationalization of the spectra as well as a benchmark to which the results obtained by other computational approaches may be compared.

Methods of Calculation

SCF Calculations and Basis Set. SCF calculations on the ground states of adenine and guanine were performed with the CADPAC system of programs[31] primarily to obtain molecular orbitals for use in the subsequent MRCI and RPA calculations. The molecules were assumed to be planar, with geometric parameters taken from the crystal structure of guanine monohydrate[32] and 9-methyladenine,[33] with minor idealizations. The molecular structures and numbering of atoms are shown in Figure 1. The basis set consisted of the Huzinaga (9s,5p/4s) primitive set of Cartesian Gaussian basis orbitals (GTOs)[34] contracted to [4s,2p/2s] double-ζ quality[35,36] along with sets of polarization and diffuse GTOs in the π system. Specifically, the polarization functions included a p_π primitive GTO with an orbital exponent of 1.0 on each hydrogen atom, and a pair of d_π primitive GTOs (i.e., d_{xz} and d_{yz} functions; see Figure 1) with exponents of 0.8 on each first-row atom. Additionally, a pair of p_π diffuse GTOs representing $n = 3$ π-type Rydberg orbitals, similar to the Rydberg basis used by Hay and Shavitt in their CI calculation on benzene,[37] were added to each first-row atom. The orbital exponents of the diffuse functions were chosen to be 10 and 30% of the smallest exponent p-type GTO of the double-ζ basis set of the atom on which they were added, giving values essentially the same as recommended by Dunning and Hay[38] for the 3p Rydberg case. The primary purpose of these latter functions was to permit investigation of the importance of $\pi \rightarrow \pi^*$ Rydberg excitations in low-lying valence (π,π^*) excited states, as well as of the possible existence of π-type Rydberg states in the spectral region under consideration. Thus, in the anticipation that (π,π^*) excited states are to be of primary importance in the present spectral studies, π orbitals of better than double-ζ quality were obtained, with orbitals of σ symmetry being determined at the double-ζ basis set level.

MRCI Calculations. The MRCI calculations were performed with programs developed locally following the method originally proposed by Whitten and Hackmeyer.[39] Details of the methodology have been presented previously,[40,41] and only an outline pertaining to the present studies will be given here. As stated above, ground-state SCF orbitals were used to describe both ground and excited states at the CI level. This means that, in principle, the ground state and excited states whose optimized orbitals closely resemble those of the ground state may be more accurately determined than other excited states. However, because of the low spatial symmetry and large number of excited states which must be obtained (see below), optimization of orbitals for each individual excited state is not a practical option.

For both adenine and guanine, the 17 highest lying occupied and 30 lowest lying unoccupied SCF orbitals were allowed variable occupancy in the CI calculations, while the remaining occupied orbitals (18 and 22 for adenine and guanine, respectively) were constrained to double occupancy in each configuration, and the higher lying unoccupied orbitals were not used in the calculations. The orbital energies and spatial characteristics of these orbitals are given in Table I. The majority of unoccupied orbitals listed are of π symmetry, although several unoccupied orbitals of σ symmetry are included as well. The values of $\langle r^2 \rangle$ in Table I show that the lowest 10 and 11 unoccupied orbitals of adenine and guanine, respectively, have extended spatial properties that would characterize them as Rydberg π^* orbitals. The lowest lying pair of unoccupied valence orbitals, labeled V_1^* and V_2^*, are much more compact, but are not as contracted as any of the high-lying occupied molecular orbitals in either molecule, owing to small

(22) Mely, B.; Pullman, A. *Theor. Chim. Acta* **1969**, *13*, 278–287.
(23) Clementi, E.; Andre, J. M.; Andre, M.; Klint, D.; Hahn, D. *Acta Phys. Acad. Sci. Hung.* **1969**, *27*, 493–521.
(24) Mezey, P. G.; Ladik, J. J. *Theor. Chim. Acta* **1979**, *52*, 129–145.
(25) Del Bene, J. E. *J. Phys. Chem.* **1983**, *87*, 367–371.
(26) Cizek, J.; Forner, W.; Ladik, J. *Theor. Chim. Acta* **1983**, *64*, 107–116.
(27) Singh, U. C.; Kollman, P. A. *J. Comput. Chem.* **1984**, *5*, 129–145.
(28) Sarai, A.; Saito, M. *Int. J. Quantum Chem.* **1984**, *25*, 527–533; **1985**, *28*, 399–409.
(29) Clementi, E.; Corongiu, G.; Detrich, J.; Chin, S.; Domingo, L. *Int. J. Quantum Chem., Quantum Chem. Symp.* **1984**, *18*, 601–618.
(30) Eisenstein, M. *Int. J. Quantum Chem.* **1988**, *33*, 127–158.
(31) Amos, R. D. CADPAC: The Cambridge Analytical Derivatives Package, Issue 2.0, Cambridge, 1986.
(32) Thewalt, U.; Bugg, C. E.; Marsh, R. E. *Acta Crystallogr.* **1971**, *B27*, 2358–2363.
(33) Stewart, R. F.; Jensen, L. H. *J. Chem. Phys.* **1964**, *40*, 2071–2075.
(34) Huzinaga, S. *J. Chem. Phys.* **1965**, *42*, 1293–1302.
(35) Dunning, T. H., Jr. *J. Chem. Phys.* **1970**, *53*, 2823–2833.
(36) In the notation $(us,vp/ws)$, u and v specify the number of s-type and p-type primitive Cartesian Gaussian functions on each first-row atom, and w gives the number of s-type primitive Cartesian Gaussian on each hydrogen atom. In the notation $[us,vp/ws]$, u, v, and w specify numbers of contracted rather than primitive functions.
(37) Hay, P. J.; Shavitt, I. *J. Chem. Phys.* **1974**, *60*, 2865–2877.
(38) Dunning, T. H., Jr.; Hay, P. J. In *Methods of Electronic Structure Theory*; Schaefer, H. F., III, Ed.; Plenum: New York, 1977.
(39) Whitten, J. L.; Hackmeyer, M. *J. Chem. Phys.* **1969**, *51*, 5584–5596.
(40) Petke, J. D.; Christoffersen, R. E.; Maggiora, G. M.; Shipman, L. L. *Int. J. Quantum Chem., Quantum Biol. Symp.* **1977**, *4*, 343–355.
(41) Petke, J. D.; Maggiora, G. M.; Shipman, L. L.; Christoffersen, R. E. *J. Mol. Spectrosc.* **1978**, *71*, 64–84.

Table I. Energies, ϵ, and Spatial Extents, $\langle r^2 \rangle$, of Occupied (1–17) and Unoccupied (1*–30*) SCF Molecular Orbitals Allowed Variable Occupancy in MRCI and RPA Calculations

adenine			guanine		
orbital[a]	ϵ[b]	$\langle r^2 \rangle$[b,c]	orbital[a]	ϵ[b]	$\langle r^2 \rangle$[b,c]
30* (σ*)	0.3517	35.0	30* (σ*)	0.3362	43.9
29* (σ*)	0.3483	38.5	29* (σ*)	0.3238	32.1
28* (σ*)	0.3312	33.5	28*	0.3074	65.3
27*	0.3236	60.9	27* (σ*)	0.2938	36.6
26* (σ*)	0.3007	41.0	26*	0.2807	65.9
25*	0.2797	66.2	25* (σ*)	0.2778	40.9
24* (σ*)	0.2763	40.2	24* (σ*)	0.2631	54.8
23*	0.2746	67.8	23*	0.2596	71.0
22* (σ*)	0.2686	38.7	22*	0.2459	73.8
21* (σ*)	0.2485	49.4	21*	0.2360	85.0
20*	0.2477	71.5	20* (σ*)	0.2330	44.8
19*	0.2372	78.0	19*	0.2030	77.7
18*	0.2014	58.3	18*	0.1964	79.2
17*	0.1845	82.3	17*	0.1912	85.3
16*	0.1830	88.6	16*	0.1788	81.7
15*	0.1802	92.1	15*	0.1618	93.7
14*	0.1683	89.6	14*	0.1563	74.8
13*	0.1439	77.8	13* (V_2*)	0.1295	70.5
12* (V_2*)	0.1282	30.7	12* (V_1*)	0.1217	30.6
11* (V_1*)	0.1045	58.5	11* (R_{11}*)	0.1118	138.3
10* (R_{10}*)	0.0890	171.1	10* (R_{10}*)	0.0967	158.9
9* (R_9*)	0.0845	162.5	9* (R_9*)	0.0779	182.4
8* (R_8*)	0.0776	154.5	8* (R_8*)	0.0729	170.8
7* (R_7*)	0.0691	165.8	7* (R_7*)	0.0692	170.5
6* (R_6*)	0.0676	158.6	6* (R_6*)	0.0598	180.1
5* (R_5*)	0.0494	212.6	5* (R_5*)	0.0491	214.0
4* (R_4*)	0.0446	253.0	4* (R_4*)	0.0415	269.8
3* (R_3*)	0.0304	241.6	3* (R_3*)	0.0342	235.0
2* (R_2*)	0.0284	244.6	2* (R_2*)	0.0259	241.2
1* (R_1*)	0.0199	210.3	1* (R_1*)	0.0169	210.3
1 (π)	−0.3265	16.5	1 (π)	−0.3067	17.8
2 (π)	−0.3696	15.7	2 (π)	−0.4124	19.4
3 (σ)	−0.3926	19.3	3 (σ)	−0.4191	21.4
4 (σ)	−0.4331	19.2	4 (σ)	−0.4307	24.2
5 (π)	−0.4335	18.0	5 (π)	−0.4428	17.9
6 (σ)	−0.4845	19.9	6 (π)	−0.4602	26.2
7 (π)	−0.5107	18.7	7 (σ)	−0.4853	18.6
8 (π)	−0.5654	19.0	8 (π)	−0.5605	20.9
9 (σ)	−0.5978	23.1	9 (σ)	−0.5948	25.3
10 (σ)	−0.6168	19.8	10 (σ)	−0.5989	26.4
11 (σ)	−0.6443	18.2	11 (π)	−0.6148	20.0
12 (π)	−0.6506	14.1	12 (σ)	−0.6367	20.2
13 (σ)	−0.6814	17.3	13 (π)	−0.6771	15.0
14 (σ)	−0.7064	26.0	14 (σ)	−0.6846	17.4
15 (σ)	−0.7504	24.3	15 (σ)	−0.7195	35.5
16 (σ)	−0.7900	22.7	16 (σ)	−0.7487	26.3
17 (σ)	−0.8500	18.5	17 (σ)	−0.7643	19.6

[a] Unoccupied orbitals are π* orbitals unless specified. [b] Atomic units. [c] Relative to the center of mass.

contributions from the diffuse p_π-type basis functions.

The CI wave function Ψ_K for state K is given by

$$\Psi_K = \sum_L C_{KL}\Phi_L \tag{1}$$

where Φ_L's are configurations constructed as linear combinations of Slater determinants of appropriate spatial and spin symmetry. The configurations were generated by making single and double excitations from a number of "parent" configurations, which were those configurations found in small exploratory CI studies to be the principal contributors (i.e., $C_{KL} > 0.20$) to the excited states of interest. The final configuration list for a given spatial symmetry and spin multiplicity consisted of those included in a 100-configuration initial CI expansion plus those generated configurations Φ_L which satisfy the criterion

$$\frac{|\langle \Phi_L|H|\Psi_M^{(0)}\rangle|^2}{|\langle \Phi_L|H|\Phi_L\rangle - E_M^{(0)}|} > \delta \tag{2}$$

for at least one initial state M, where H is the molecular electronic Hamiltonian operator, $\Psi_M^{(0)}$ and $E_M^{(0)}$ are the Mth wave function and energy, respectively, of the 100-configuration initial exploratory CI, and δ is a threshold value set at 10^{-4} hartree. Generally, final configuration lists (for a given spatial symmetry and spin multiplicity) consisted of approximately 5000 singly, doubly, triply, and quadruply excitated configurations relative to the ground-state SCF configuration. At the present level of computation, the majority of excitations are of the $\pi \rightarrow \pi^*$ or $\sigma \rightarrow \pi^*$ type (depending on the spatial symmetry of a given state), although $\sigma \rightarrow \sigma^*$ and $\pi \rightarrow \sigma^*$ excitations are also present to a limited degree.

Final MRCI wave functions Ψ_K and energies E_K were determined from the usual linear variational equations

$$\sum_L (H_{JL} - \delta_{JL}E_K)C_{KL} = 0 \tag{3}$$

where the Hamiltonian matrix elements, H_{JL}, are given by

$$H_{JL} = \langle \Phi_J|H|\Phi_L\rangle \tag{4}$$

The roots of the Hamiltonian matrix were found using the Davidson iterative method.[42]

The transition dipole for the electronic excitation from the ground-state Ψ_0 to excited state Ψ_K is

$$\langle \Psi_0|\mathbf{r}|\Psi_K\rangle = \sum_M \sum_N C_{M0}C_{NK}\langle \Phi_M|\mathbf{r}|\Phi_N\rangle \tag{5}$$

which may be approximated by

$$\langle \Psi_0|\mathbf{r}|\Psi_K\rangle \simeq C_{00}\sum_N C_{NK}\langle \Phi_0|\mathbf{r}|\Phi_N\rangle \tag{6}$$

since the ground-state wave function is dominated by the SCF configuration Φ_0 with $C_{00} \approx 0.95$. In eq 6, matrix elements $\langle \Phi_0|\mathbf{r}|\Phi_N\rangle$ are zero unless $\Phi_N = \Phi(i \rightarrow a)$ is a singly excited configuration relative to Φ_0, the excitation being from occupied SCF molecular orbital φ_i to unoccupied orbital φ_a. Evaluation of the nonzero matrix elements leads to the expression

$$\langle \Psi_0|\mathbf{r}|\Psi_K\rangle \simeq 2^{1/2}C_{00}\sum_i \sum_a C_K(i \rightarrow a)\langle \varphi_i|\mathbf{r}|\varphi_a\rangle \tag{7}$$

where the summations are carried out over the occupied and unoccupied molecular orbitals having variable occupancy in the MRCI calculation, and $C_K(i \rightarrow a) = C_{NK}$ is the expansion coefficient of $\Phi(i \rightarrow a)$ in Ψ_K. This equation will be used for an analysis of computed oscillator strengths.

RPA Calculations. RPA studies were performed with the method developed by Bouman and Hansen, which has been presented in detail in previous publications.[43–45] The calculations were carried out with the RPAC program[46] obtained from the Quantum Chemistry Program Exchange (QCPE 459) and modified to interface with local SCF and MRCI codes.

The RPA method is one of a number of "equations of motion" methods[47,48] in which transition energies ΔE_{0K} and intensities are obtained directly, thus avoiding the necessity of obtaining explicit ground- and excited-state wave functions. The RPA method gives the correct linear response of a closed-shell SCF ground state to an external perturbation, the excited state being given implicitly as a linear combination of singly excited configurations. The transition energies are obtained as roots of the non-Hermitian matrix equations

$$\begin{bmatrix} \mathbf{A} & \mathbf{B} \\ -\mathbf{B} & -\mathbf{A} \end{bmatrix}\begin{bmatrix} \mathbf{X}_K \\ \mathbf{Y}_K \end{bmatrix} = \Delta E_{0K}\begin{bmatrix} \mathbf{X}_K \\ \mathbf{Y}_K \end{bmatrix} \tag{8}$$

The symmetric matrices $\mathbf{A}$ and $\mathbf{B}$ are of dimension equal to the number of singly excited configurations, and are given by

$$\mathbf{A}_{ia,jb} = \langle \Phi(i \rightarrow a)|H|\Phi(j \rightarrow b)\rangle - \delta_{ij}\delta_{ab}\langle \Phi_0|H|\Phi_0\rangle \tag{9}$$

and

$$\mathbf{B}_{ia,jb} = \langle \Phi(i \rightarrow a, j \rightarrow b)|H|\Phi_0\rangle \tag{10}$$

where Φ_0 is the ground-state SCF configuration, $\Phi(i \rightarrow a)$ is a singly

(42) Davidson, E. R. *J. Comput. Phys.* **1975**, *17*, 87–94.
(43) Bouman, T. D.; Hansen, A. E. *J. Chem. Phys.* **1977**, *66*, 3460–3467.
(44) Hansen, A. E.; Bouman, T. D. *Adv. Chem. Phys.* **1980**, *44*, 545–644.
(45) Hansen, A. E.; Bouman, T. D. *J. Am. Chem. Soc.* **1985**, *107*, 4828–4839.
(46) Bouman, T. D.; Hansen, A. E.; Voigt, B.; Rettrup, S. *Int. J. Quantum Chem.* **1983**, *23*, 595–611. *QCPE Bull.* **1983**, QCPE 459.
(47) Dunning, T. H.; McKoy, V. *J. Chem. Phys.* **1967**, *47*, 1735–1747.
(48) Shibuya, T.; Rose, J.; McKoy, V. *J. Chem. Phys.* **1973**, *58*, 500–507.

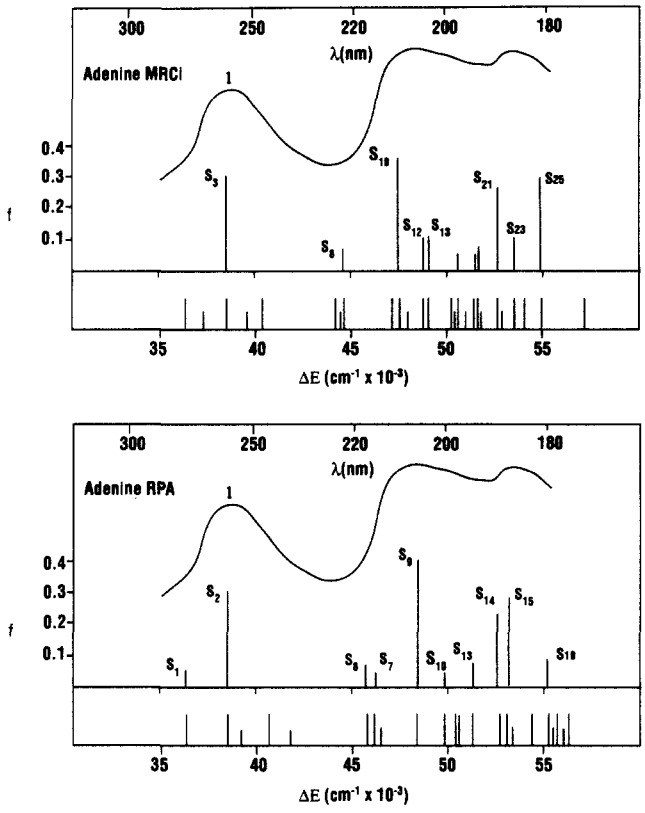

Figure 2. Comparison of the experimental absorption spectrum of adenine (adapted from ref 6) with calculated transitions from MRCI and RPA studies. Calculated energies are scaled transition energies (see ref 48), and f is the calculated oscillator strength. Transitions with $f > 0.05$ are labeled denoting the relevant excited state and are shown below the experimental spectrum; vertical lines give calculated values of f. At the bottom of each figure, the location of all calculated transitions is shown, with full- and half-height vertical lines representing $\pi \rightarrow \pi^*$ and $\sigma \rightarrow \pi^*$ transitions, respectively.

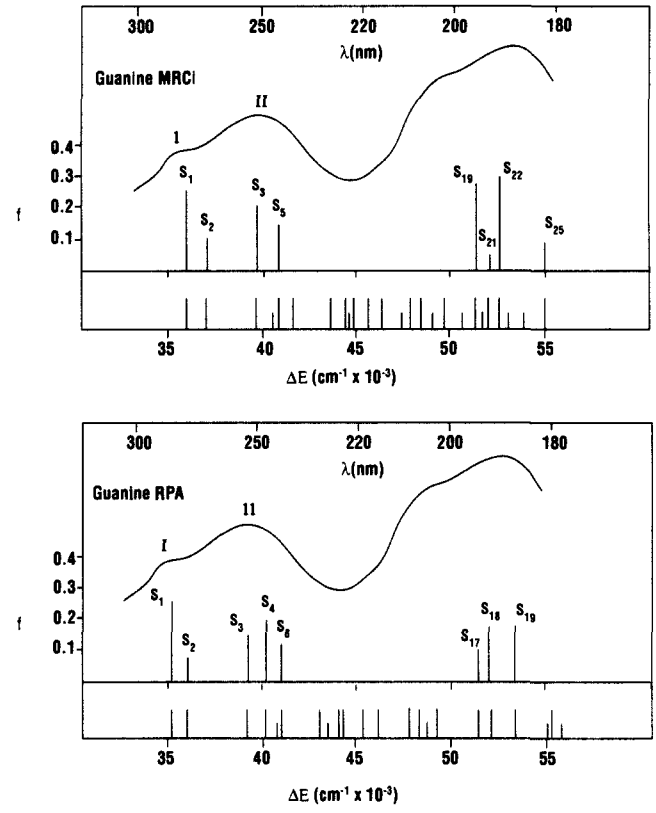

Figure 3. Comparison of the experimental absorption spectrum of guanine (adapted from ref 6) with calculated transitions from MRCI and RPA studies. The notation is the same as for Figure 2.

excitated configuration, and $\Phi(i \rightarrow a, j \rightarrow b)$ is a doubly excited configuration, the excitations being from orbitals φ_i to φ_a and φ_j to φ_b, respectively. The matrix **B** given in eq 10 is associated with the implicit inclusion of ground-state correlation due to the presence of doubly excited configurations relative to Φ_0.

The transition dipole is given by an equation similar in form to eq 7,

$$\langle \Psi_0 | \mathbf{r} | \Psi_K \rangle = 2^{1/2} \sum_i \sum_a \{X_{ia,K} + Y_{ia,K}\} \langle \varphi_i | \mathbf{r} | \varphi_a \rangle \qquad (11)$$

where the eigenvector coefficients $\{X_{ia,K} + Y_{ia,K}\}$ are obtained from the Kth root of eq 8. For the present RPA studies, the SCF orbitals employed are the same 47 molecular orbitals allowed variable occupancy in the CI calculations. Solution of eq 8 was obtained with the Jorgensen–Linderberg method.[49]

Results and Discussion: Excited States and Spectra

In the present MRCI calculations, excited singlet states sufficient in number to account for the absorption spectra up to approximately 55 000 cm^{-1} were obtained. The selection of these states was based on two considerations. First, it was expected that calculated transition energies would be high relative to experimental values by 8000–12 000 cm^{-1} (1–1.5 eV), as was the case in a study of benzene performed at a similar level of theory by Hay and Shavitt.[37] Second, calculated oscillator strengths were examined to ensure that a sufficient number of states was obtained to provide a general "fit" of the experimental spectra in all regions of intense absorption between 35 000 and 55 000 cm^{-1}. In fact, the calculated transition energies were found on average to be 12 000–15 000 cm^{-1} higher than experimental values, and there are at least 20–25 calculated excited singlet states which contribute to the spectra in the region of interest. Calculated data, including transition energies, oscillator strengths, polarizations, dipole moments, and second moments of the charge distribution are given in Table II. MRCI calculations of a number of low-lying triplet states of adenine and guanine were also performed, and the resulting data may be found in Table III.

In the RPA studies, similar guidelines were followed, but it was thought that transition energy errors would be smaller than in the MRCI studies, based on general trends in previous work by Hansen and Bowman.[45] However, in the present case the average transition energy errors from both the MRCI and RPA studies were found to be similar. It should be noted that the present RPA calculations employed a truncated set of virtual orbitals, whereas previous RPA studies on smaller molecules (e.g., twisted ethylene and *trans* 2-butene) used all virtual orbitals provided by the basis set employed.[43,45] In the RPA calculations on cytosine reported by Jensen et al.,[8] however, a full set of virtual orbitals was used, yet relatively large transition energy errors averaging 10 000 cm^{-1} were obtained. Thus, use of a full virtual orbital set is apparently not sufficient to substantially reduce errors in calculated transition energies in extremely complex molecules such as the purine and pyrimidine bases. Table IV contains calculated data from the RPA studies of adenine and guanine.

Before proceeding with a more detailed analysis, several general comments are appropriate. First, in order to present a more informative qualitative picture of the relation of the present results to experimental spectra, Figures 2 and 3 compare the experimental spectra of adenine and guanine with calculated spectra obtained by linearly scaling the calculated transition energies.[50] For such

(49) Jorgensen, P.; Linderberg, J. *Int. J. Quantum Chem.* **1970**, *4*, 587–602.

(50) The scaling of calculated transition energies was done using linear equations constructed by assigning two absorption maxima to appropriate calculated transition energies. In adenine, the maxima at 38 610 and 53 190 cm^{-1} were assigned to the ($S_0 \leftarrow S_3$) transition, and the average of the ($S_0 \leftarrow S_{21}$) and ($S_0 \leftarrow S_{23}$), transitions, respectively (MRCI), and to the ($S_0 \leftarrow S_2$) transition, and the average of the ($S_0 \leftarrow S_{14}$) and ($S_0 \leftarrow S_{15}$) transitions, respectively (RPA). For guanine, maxima at 39 525 and 52 910 cm^{-1} were assigned to the ($S_0 \leftarrow S_3$) and ($S_0 \leftarrow S_{22}$) transitions, respectively, (MRCI), and to the ($S_0 \leftarrow S_3$) and ($S_0 \leftarrow S_{18}$) transitions (RPA).

Table II. Transition Energies, Oscillator Strengths, f, Dipole Moments, μ, and $\langle z^2 \rangle$ of the Electron Distribution of Adenine and Guanine Singlet States, Obtained from MRCI Calculations

state[a]	transition energy[c] calcd (scaled)	f (θ)[d]	μ (θ)[d,e]	$\langle z^2 \rangle$[f]
		Adenine		
S_0	0.0		2.68 (−84)	45.7
S_1	51 280 (36 310)	0.001 (−33)	2.97 (−73)	47.3
S_2[b]	52 341 (37 260)	0.003	1.03 (156)	48.4
S_3	53 849 (38 610)	0.318 (+41)	1.70 (−69)	51.0
S_4[b]	54 922 (39 570)	0.004	1.42 (0)	48.6
S_5	55 748 (40 310)	0.003 (−54)	1.41 (55)	113.7
S_6	60 339 (44 420)	0.011	2.33 (−126)	109.9
S_7[b]	60 709 (44 750)	0.010	2.71 (−59)	49.1
S_8	60 774 (44 810)	0.071 (−48)	4.64 (−22)	113.3
S_9	63 724 (47 450)	0.003	3.06 (60)	119.8
S_{10}	64 188 (47 860)	0.372 (−68)	2.10 (−114)	83.0
S_{11}[b]	64 465 (48 110)	0.000	0.81 (−47)	110.8
S_{12}	65 381 (48 930)	0.119 (−58)	3.55 (−28)	109.5
S_{13}	65 607 (49 130)	0.110 (−82)	7.51 (−111)	107.4
S_{14}	66 773 (50 180)	0.075 (−57)	5.91 (−25)	157.8
S_{15}[b]	67 051 (50 430)	0.034	2.55 (−114)	50.8
S_{16}	67 486 (50 820)	0.056 (−22)	9.58 (−81)	114.5
S_{17}[b]	67 769 (51 070)	0.000	3.09 (−113)	48.9
S_{18}	68 587 (51 800)	0.054 (−23)	3.69 (−113)	126.7
S_{19}	68 676 (51 880)	0.081 (+62)	2.74 (−63)	111.4
S_{20}[b]	68 724 (51 920)	0.004	2.78 (71)	118.2
S_{21}	69 667 (52 770)	0.227 (+9)	4.64 (−62)	87.6
S_{22}[b]	69 900 (52 980)	0.000	0.67 (−86)	134.4
S_{23}	70 609 (53 610)	0.101 (−60)	6.04 (−9)	105.1
S_{24}	71 257 (54 190)	0.035	1.52 (−44)	126.9
S_{25}	72 167 (55 000)	0.310 (+38)	3.99 (−94)	62.5
S_{26}	74 650 (57 230)	0.016	1.80 (−124)	58.5
		Guanine		
S_0	0.0		7.89 (158)	49.3
S_1	49 709 (35 790)	0.239 (−52)	5.41 (−156)	66.2
S_2	51 175 (36 880)	0.088 (+3)	5.79 (125)	87.4
S_3	54 716 (39 525)	0.216 (+80)	6.29 (172)	84.1
S_4[b]	55 965 (40 460)	0.002	5.56 (115)	51.9
S_5	56 179 (40 620)	0.136 (+51)	5.27 (146)	92.0
S_6	57 436 (41 560)	0.019	3.61 (150)	109.3
S_7	60 262 (43 670)	0.002	4.79 (121)	125.1
S_8	61 530 (44 610)	0.002	9.82 (163)	132.9
S_9[b]	61 750 (44 780)	0.015	6.75 (150)	53.2
S_{10}	61 774 (44 800)	0.003	7.57 (−173)	147.5
S_{11}	63 080 (45 770)	0.019	12.09 (170)	105.2
S_{12}	64 039 (46 490)	0.002	5.06 (120)	146.3
S_{13}[b]	65 430 (47 530)	0.005	6.93 (−169)	53.1
S_{14}	66 117 (48 040)	0.043	5.75 (158)	93.0
S_{15}	66 803 (48 550)	0.005	4.71 (173)	120.4
S_{16}[b]	67 681 (49 210)	0.000	1.83 (−57)	86.7
S_{17}	68 403 (49 740)	0.033	14.27 (146)	118.2
S_{18}[b]	70 049 (50 970)	0.000	0.73 (123)	94.4
S_{19}	70 865 (51 580)	0.228 (+73)	12.13 (−172)	87.0
S_{20}[b]	71 510 (52 060)	0.003	2.00 (49)	125.5
S_{21}	71 824 (52 300)	0.048 (+64)	2.28 (79)	116.1
S_{22}	72 643 (52 910)	0.297 (+73)	11.61 (−179)	84.2
S_{23}[b]	73 190 (53 320)	0.000	9.36 (59)	139.5
S_{24}[b]	74 320 (54 160)	0.000	4.77 (114)	135.0
S_{25}	75 566 (55 090)	0.091 (+77)	6.55 (171)	61.0

[a] (π,π^*) unless specified. [b] (σ,π^*). [c] In cm^{-1}. See ref 48 for scaling details. [d] Polarization angle defined in Figure 1. [e] In debye; vector points negative to positive. [f] In atomic units, relative to the center of mass.

Table III. Transition Energies, Dipole Moments, μ, and $\langle z^2 \rangle$ of the Electron Distribution of Adenine and Guanine Triplet States, Obtained from MRCI Calculations

state[a]	transition energy[c] calcd (scaled)	μ (θ)[d,e]	$\langle z^2 \rangle$[f]
	Adenine		
T_1	38 562 (24 930)	1.54 (−52)	47.2
T_2	46 311 (31 860)	4.27 (−65)	47.1
T_3	48 397 (33 730)	2.68 (−84)	48.5
T_4	50 328 (35 460)	4.45 (−39)	48.5
T_5[b]	50 924 (35 990)	1.39 (161)	48.6
T_6[b]	52 769 (37 640)	1.89 (3)	49.2
T_7	53 612 (38 400)	2.08 (−87)	48.7
T_8	55 345 (39 950)	1.50 (51)	106.5
T_9[b]	57 436 (41 820)	8.42 (124)	50.5
T_{10}	59 661 (43 810)	2.60 (−151)	109.1
T_{11}	60 985 (45 000)	3.92 (−32)	115.9
T_{12}[b]	63 719 (47 440)	9.14 (−75)	52.3
T_{13}	63 759 (47 480)	3.27 (77)	114.3
T_{14}[b]	64 426 (48 080)	1.22 (−56)	110.6
T_{15}	64 526 (48 170)	0.28 (−109)	114.0
T_{16}	65 340 (48 900)	4.82 (−116)	138.4
T_{17}	65 780 (49 290)	1.00 (−80)	81.9
T_{18}	66 084 (49 560)	8.63 (−41)	132.7
T_{19}[b]	66 442 (49 880)	8.98 (−74)	50.2
T_{20}	67 552 (50 880)	10.36 (−83)	111.9
T_{21}	68 161 (51 420)	2.35 (−145)	124.0
T_{22}	68 513 (51 740)	5.77 (−94)	141.6
T_{23}[b]	68 663 (51 870)	2.82 (67)	119.2
T_{24}[b]	68 886 (52 960)	0.74 (−77)	134.4
T_{25}	70 124 (53 180)	7.44 (−29)	127.8
T_{26}[b]	73 202 (55 930)	1.91 (−106)	128.0
	Guanine		
T_1	39 647 (28 280)	7.81 (180)	50.2
T_2	41 311 (29 520)	12.39 (138)	52.3
T_3	49 313 (35 490)	6.48 (180)	56.6
T_4	51 938 (37 450)	3.29 (161)	108.0
T_5[b]	54 470 (39 340)	5.98 (108)	53.4
T_6	55 436 (40 060)	2.26 (164)	108.8
T_7[b]	57 178 (41 360)	13.61 (142)	57.1
T_8	57 702 (41 760)	5.45 (−175)	116.0
T_9	60 322 (43 710)	7.89 (118)	109.5
T_{10}	61 453 (44 560)	10.60 (174)	124.8
T_{11}	61 752 (44 780)	9.08 (151)	75.5
T_{12}	62 090 (45 030)	4.40 (171)	165.8
T_{13}	64 039 (46 490)	9.05 (176)	141.7
T_{14}	64 344 (46 710)	5.69 (−165)	113.8
T_{15}[b]	64 537 (46 860)	6.86 (−106)	54.0
T_{16}	65 045 (47 240)	8.01 (−160)	67.5
T_{17}	66 868 (48 600)	4.07 (173)	124.8
T_{18}	67 123 (48 790)	7.18 (139)	82.1
T_{19}[b]	67 579 (49 130)	3.10 (−45)	83.5
T_{20}	67 972 (49 420)	11.87 (136)	116.8
T_{21}[b]	69 867 (50 840)	0.67 (−30)	95.5
T_{22}[b]	71 527 (52 080)	0.89 (49)	118.4

[a] (π,π^*) unless specified. [b] (σ,π^*). [c] In cm^{-1}. See ref 48 for scaling details. [d] In debye; vector points negative to positive. [e] Polarization angle θ defined in Figure 1. [f] In atomic units, relative to the center of mass.

a procedure to be valid, errors in calculated transition energies must be approximately the same for all states, and this has not been the case in a number of previously reported studies, where accurate individual transition energies obtained from high resolution experimental spectra are available for direct comparison with calculated results. For example, in CI studies of benzene[37,51,52] and butadiene[53-55] transition energy errors were found to be within a range of 0–16 000 cm^{-1} (0–2 eV), with the transition energies of excited states having "covalent" charge distributions being more accurately calculated than those with more "ionic" charge distributions.

In adenine and guanine, however, the available experimental spectra obtained in solution have not been resolved into specific electronic transitions, and detailed comparisons between experimental and calculated transition energies are not possible. Nevertheless, assignments of calculated intense transitions to the major broad-banded regions of absorption can be made. In doing so, an approximate linear relationship between calculated transition

(51) Peyerimhoff, S. D.; Buenker, R. J. *Theor. Chim. Acta* **1970**, *19*, 1–19.
(52) Matos, J. M. O.; Roos, B.; Malmqvist, P.-A. *J. Chem. Phys.* **1987**, *86*, 1458–1466.
(53) Buenker, R. J.; Whitten, J. L. *J. Chem. Phys.* **1968**, *49*, 5381–5387.
(54) Hosteny, R. P.; Dunning, T. H.; Gilman, R. R.; Pipano, A.; Shavitt, I. *J. Chem. Phys.* **1975**, *62*, 4764–4779.
(55) Cave, R. J.; Davidson, E. R. *J. Phys. Chem.* **1987**, *91*, 4481–4490.

Table IV. Transition Energies, Oscillator Strengths, f, and Polarizations, θ, of Singlet–Singlet Transitions of Adenine and Guanine Obtained from RPA Calculations

transition[a]	transition energy[c] calcd (scaled)	f (θ)[d]
	Adenine	
$S_1 \leftarrow S_0$	51 861 (36 300)	0.059 (+35)
$S_2 \leftarrow S_0$	54 107 (38 620)	0.332 (+51)
$S_3 \leftarrow S_0$[b]	54 733 (39 260)	0.002
$S_4 \leftarrow S_0$	56 128 (40 700)	0.005
$S_5 \leftarrow S_0$[b]	57 300 (41 910)	0.005
$S_6 \leftarrow S_0$	61 141 (45 880)	0.121 (−57)
$S_7 \leftarrow S_0$	61 544 (46 300)	0.050 (−33)
$S_8 \leftarrow S_0$[b]	61 708 (46 470)	0.013
$S_9 \leftarrow S_0$	63 815 (48 640)	0.437 (−59)
$S_{10} \leftarrow S_0$	65 095 (49 970)	0.052 (−71)
$S_{11} \leftarrow S_0$	65 662 (50 550)	0.013
$S_{12} \leftarrow S_0$	65 898 (50 800)	0.015
$S_{13} \leftarrow S_0$	66 672 (51 600)	0.089 (−51)
$S_{14} \leftarrow S_0$	67 912 (52 880)	0.251 (+21)
$S_{15} \leftarrow S_0$	68 518 (53 500)	0.315 (+58)
$S_{16} \leftarrow S_0$[b]	68 546 (53 530)	0.023
$S_{17} \leftarrow S_0$	69 772 (54 750)	0.015
$S_{18} \leftarrow S_0$	70 084 (55 120)	0.110 (+18)
$S_{19} \leftarrow S_0$[b]	70 554 (55 610)	0.000
$S_{20} \leftarrow S_0$	70 807 (55 870)	0.008
$S_{21} \leftarrow S_0$[b]	70 962 (56 030)	0.001
$S_{22} \leftarrow S_0$	71 297 (56 370)	0.013
	Guanine	
$S_1 \leftarrow S_0$	50 241 (35 410)	0.266 (−46)
$S_2 \leftarrow S_0$	51 352 (36 260)	0.069 (+13)
$S_3 \leftarrow S_0$	55 597 (39 525)	0.159 (+87)
$S_4 \leftarrow S_0$	57 066 (40 650)	0.212 (+60)
$S_5 \leftarrow S_0$[b]	57 724 (41 160)	0.002
$S_6 \leftarrow S_0$	57 866 (41 270)	0.140 (+69)
$S_7 \leftarrow S_0$	60 418 (43 230)	0.008
$S_8 \leftarrow S_0$[b]	61 090 (43 740)	0.018
$S_9 \leftarrow S_0$	61 714 (44 220)	0.003
$S_{10} \leftarrow S_0$	62 234 (44 620)	0.030
$S_{11} \leftarrow S_0$	63 323 (45 460)	0.014
$S_{12} \leftarrow S_0$	64 422 (46 300)	0.008
$S_{13} \leftarrow S_0$	66 617 (47 990)	0.014
$S_{14} \leftarrow S_0$	67 272 (48 490)	0.008
$S_{15} \leftarrow S_0$[b]	67 579 (48 730)	0.005
$S_{16} \leftarrow S_0$	68 544 (49 470)	0.042 (+67)
$S_{17} \leftarrow S_0$	72 272 (52 330)	0.122 (+82)
$S_{18} \leftarrow S_0$	73 026 (52 910)	0.203 (+80)
$S_{19} \leftarrow S_0$	74 661 (54 170)	0.198 (+86)
$S_{20} \leftarrow S_0$[b]	75 814 (55 050)	0.016
$S_{21} \leftarrow S_0$	75 902 (55 120)	0.005
$S_{22} \leftarrow S_0$[b]	76 680 (55 720)	0.003

[a] ($\pi \rightarrow \pi^*$) unless specified. [b] ($\sigma \rightarrow \pi^*$). [c] In cm^{-1}. See ref 48 for scaling details. [d] Polarization angle defined in Figure 1.

energies and experimental absorption maxima is evident, with transition energy errors within a range of 12 000–15 000 cm^{-1}. Thus, a formal linear scaling of the present calculated transition energies appears to be appropriate for providing a consistent qualitative picture of the spectral features of the low resolution spectra of adenine and guanine, as indicated in Figures 2 and 3.

It is clear from these figures and the data in Tables II and IV that for both molecules a large number of closely spaced transitions of varying intensity contribute to the spectral region between 35 000 and 55 000 cm^{-1}. The number of calculated transitions in this region is much larger than has been previously reported in semiempirical studies.[8-21] This may be attributed primarily to the presence of Rydberg π^* virtual orbitals in the molecular basis, which provide the opportunity for describing both additional Rydberg excited states and mixed valence/Rydberg states, neither of which is usually accounted for in semiempirical methods. Another factor contributing to the complexity of the calculated spectra is the low spatial symmetry of each molecule, which permits both more extensive configuration mixing as well as more mixing among groups of nearly degenerate electronic states than is allowed in systems of higher symmetry, such as butadiene and benzene. It follows that a precise resolution of all regions of the spectra of the present systems cannot be obtained from the present calculations, particularly in the higher energy regions where differences occur between the results obtained from the RPA and MRCI methods. However, in the lower energy region of the spectra, between 35 000 and 42 000 cm^{-1}, there are clear correlations between transitions obtained from the MRCI and RPA calculations, and specific comments on the constituent transitions of this spectral region for each molecule are given below.

Adenine: Band I. In adenine, the lowest energy region of absorption at 38 500 cm^{-1} (260 nm), band I, has been shown by MCD,[56] CD,[57,58] and other methods[6,59] to consist of two or possibly more individual electronic transitions. In general, most semiempirical SCF/CI studies of adenine have predicted a pair of closely spaced $\pi \rightarrow \pi^*$ transitions in this region, only one of which is intense.[6] In the present studies, both MRCI and RPA methods are consistent in predicting five individual singlet–singlet transitions. However, two of these are weak $\sigma \rightarrow \pi^*$ transitions and another ($S_5 \leftarrow S_0$ (MRCI); $S_4 \leftarrow S_0$ (RPA)) is a $\pi \rightarrow \pi^*$ transition involving a Rydberg-like excited state with a charge distribution considerably more diffuse than that of the ground state (see Tables II and IV), and an inherently low oscillator strength. The remaining two $\pi \rightarrow \pi^*$ transitions ($S_1 \leftarrow S_0$ and $S_3 \leftarrow S_0$ (MRCI); $S_1 \leftarrow S_0$ and $S_2 \leftarrow S_0$ (RPA)) involve valence excited states with values of $\langle z^2 \rangle$ similar to that of the ground state. Since only one of the latter valence $\pi \rightarrow \pi^*$ transitions is intense, the present result appear to predict that the intensity of band I arises essentially from a single $\pi \rightarrow \pi^*$ transition, as is predicted in most semiempirical studies. Table V lists singly excited configurations $\Phi(i \rightarrow a)$ associated with the matrix elements $\langle \varphi_i | r | \varphi_a \rangle$ which have the largest coefficients in the expansion of the transition dipoles (eq 7 and 11) of the three $\pi \rightarrow \pi^*$ transitions of band I. Clearly, there is a high degree of similarity in the weighting of each configuration in the respective MRCI and RPA results.

There has been no agreement to date between theoretical predictions and experimental measurements regarding the polarization of band I. Stewart and Jensen[33] performed polarized absorption experiments on adenine crystals and determined two possible transition moment directions consistent with the dichroic ratio, $\theta = -3°$ and $\theta = +45°$ (see Figure 1). However, in considering the earlier polarized absorption studies of Stewart and Davidson[60] on thymine and thymine–adenine dimer single crystals, they determined that only the former value was consistent with the experimental data of both studies. Subsequently, Matsouka and Norden[59] performed linear dichroism measurements of adenine on stretched poly(vinyl alcohol) films and found $\theta = +9°$ or $\theta = -70°$, the former value essentially in agreement with the crystal value. Recently, however, Clark[61] has questioned these assignments, based on the polarized reflectance spectrum of 6-(methylamino)purine crystals, in which a pair of transitions was detected at 286 nm ($f = 0.10$, $\theta = +83°$) and 270 nm ($f = 0.22$, $\theta = +25°$), respectively. In contrast, the present work precicts a value of $\theta = +41°$ for the intense ($S_3 \leftarrow S_0$) transition (MRCI), and $\theta = +51°$ for the corresponding ($S_2 \leftarrow S_0$) transition (RPA),[62] which coincidently agree with the $\theta = +45°$ value rejected by Stewart and Jensen.[33] Moreover, a number of semiempirical studies[13,14,16,20,21] also predict the polarization of band I to be in the range of $\theta = +40°$ to $\theta = +70°$ (an exception is ref 15 where $\theta = +155°$).

In considering this problem, we can find no plausible reason why either the theoretical or experimental values of the polarization of band I should be grossly in error. In fact, we believe

(56) Voelter, W.; Records, R.; Bunnenberg, E.; Djerassi, C. *J. Am. Chem. Soc.* **1968**, *90*, 6163–6170.
(57) Brunner, W. C.; Maestre, M. F. *Biopolymers* **1975**, *14*, 555–565.
(58) Fornaserio, D.; Roos, I. A. G.; Rye, K.-A.; Kurucsev, T. *J. Am. Chem. Soc.* **1981**, *103*, 1908–1913.
(59) Matsuoka, Y.; Norden, B. *J. Phys. Chem.* **1982**, *86*, 1378–1386.
(60) Stewart, R. F.; Davidson, N. *J. Chem. Phys.* **1963**, *39*, 255–266.
(61) Clark, L. B. *J. Phys. Chem.* **1989**, *93*, 5345–5347.
(62) The values of θ appear to be stable with respect to the method of calculation of the transition dipole: reported values obtained from transition dipoles obtained with the "length" operator (eq 5 and 11) agreed with those obtained with the "velocity" operator (not reported) to within 3°.

Table V. Contributions of Principal Single Excitations to the Intensities of Selected ($\pi \rightarrow \pi^*$) Transitions in Adenine and Guanine[a]

MRCI[b]		RPA[c]	
		Adenine	
$S_1 \leftarrow S_0$	−0.01 ($1 \rightarrow V_1^*$)	$S_1 \leftarrow S_0$	0.24 ($1 \rightarrow V_1^*$)
	−0.53 ($2 \rightarrow V_1^*$)		−0.52 ($2 \rightarrow V_1^*$)
	0.67 ($1 \rightarrow V_2^*$)		0.68 ($1 \rightarrow V_2^*$)
	0.05 ($2 \rightarrow V_2^*$)		
$S_3 \leftarrow S_0$	0.66 ($1 \rightarrow V_1^*$)	$S_2 \leftarrow S_0$	0.64 ($1 \rightarrow V_1^*$)
	0.05 ($2 \rightarrow V_1^*$)		0.18 ($2 \rightarrow V_1^*$)
	−0.01 ($1 \rightarrow V_2^*$)		−0.29 ($1 \rightarrow V_2^*$)
	0.30 ($2 \rightarrow V_2^*$)		0.32 ($2 \rightarrow V_2^*$)
	0.26 ($1 \rightarrow R_2^*$)		0.22 ($1 \rightarrow R_2^*$)
	0.29 ($1 \rightarrow R_7^*$)		0.26 ($1 \rightarrow R_7^*$)
	−0.39 ($1 \rightarrow R_8^*$)		−0.34 ($1 \rightarrow R_8^*$)
$S_5 \leftarrow S_0$	0.83 ($1 \rightarrow R_1^*$)	$S_4 \leftarrow S_0$	0.79 ($1 \rightarrow R_1^*$)
	0.41 ($1 \rightarrow R_6^*$)		0.50 ($1 \rightarrow R_6^*$)
	−0.14 ($1 \rightarrow R_5^*$)		−0.18 ($1 \rightarrow R_5^*$)
		Guanine	
$S_1 \leftarrow S_0$	0.64 ($1 \rightarrow V_1^*$)	$S_1 \leftarrow S_0$	0.71 ($1 \rightarrow V_1^*$)
	0.48 ($1 \rightarrow R_1^*$)		0.40 ($1 \rightarrow R_1^*$)
	0.41 ($1 \rightarrow R_6^*$)		0.38 ($1 \rightarrow R_6^*$)
	0.19 ($1 \rightarrow V_2^*$)		0.15 ($1 \rightarrow V_2^*$)
$S_2 \leftarrow S_0$	−0.58 ($1 \rightarrow R_1^*$)	$S_2 \leftarrow S_0$	−0.61 ($1 \rightarrow R_1^*$)
	0.50 ($1 \rightarrow V_1^*$)		0.40 ($1 \rightarrow V_1^*$)
	0.33 ($1 \rightarrow R_8^*$)		0.35 ($1 \rightarrow R_8^*$)
	0.29 ($1 \rightarrow R_2^*$)		0.32 ($1 \rightarrow R_2^*$)
	−0.24 ($1 \rightarrow R_6^*$)		−0.31 ($1 \rightarrow R_6^*$)
	0.15 ($1 \rightarrow R_{11}^*$)		0.13 ($1 \rightarrow R_{11}^*$)
	0.14 ($1 \rightarrow R_9^*$)		0.16 ($1 \rightarrow R_9^*$)
	−0.11 ($1 \rightarrow V_2^*$)		−0.11 ($1 \rightarrow V_2^*$)
$S_3 \leftarrow S_0$	−0.49 ($1 \rightarrow R_2^*$)	$S_3 \leftarrow S_0$	−0.64 ($1 \rightarrow R_2^*$)
	0.48 ($1 \rightarrow V_2^*$)		0.35 ($1 \rightarrow V_2^*$)
	−0.32 ($1 \rightarrow R_1^*$)		−0.34 ($1 \rightarrow R_1^*$)
	−0.30 ($1 \rightarrow R_8^*$)		−0.33 ($1 \rightarrow R_8^*$)
	−0.27 ($1 \rightarrow R_{11}^*$)		−0.18 ($1 \rightarrow R_{11}^*$)
	0.22 ($1 \rightarrow V_1^*$)		0.25 ($1 \rightarrow V_1^*$)
$S_5 \leftarrow S_0$	0.62 ($1 \rightarrow R_2^*$)	$S_4 \leftarrow S_0$	0.35 ($1 \rightarrow R_2^*$)
	0.40 ($1 \rightarrow V_2^*$)		0.39 ($1 \rightarrow V_2^*$)
	−0.32 ($1 \rightarrow R_{11}^*$)		−0.33 ($1 \rightarrow R_{11}^*$)
	−0.22 ($1 \rightarrow R_3^*$)		−0.54 ($1 \rightarrow R_3^*$)
	−0.19 ($1 \rightarrow V_1^*$)		
$S_6 \leftarrow S_0$	−0.79 ($1 \rightarrow R_3^*$)	$S_6 \leftarrow S_0$	−0.65 ($1 \rightarrow R_3^*$)
	0.29 ($1 \rightarrow R_7^*$)		0.19 ($1 \rightarrow R_7^*$)
	−0.25 ($1 \rightarrow V_2^*$)		−0.43 ($1 \rightarrow V_2^*$)
	−0.24 ($1 \rightarrow R_{10}^*$)		−0.19 ($1 \rightarrow R_{10}^*$)
	−0.16 ($1 \rightarrow R_2^*$)		−0.36 ($1 \rightarrow R_2^*$)
	0.15 ($1 \rightarrow R_1^*$)		0.12 ($1 \rightarrow R_1^*$)
	0.12 ($1 \rightarrow V_1^*$)		0.17 ($1 \rightarrow V_1^*$)

[a] Excitations refer to molecular orbitals listed in Table I. [b] Coefficients given are $C_K(i \rightarrow a)$ in eq 7. [c] Coefficients given are $\{X_{ia,K} + Y_{ia,K}\}$ in eq 11.

that both values are correct; i.e., the actual polarization of band I probably varies considerably with the molecular environment and cannot be expected to maintain a single value in a variety of environmental situations. The possibility that gas-phase and condensed-phase polarizations differ significantly has been mentioned previously by Callis,[21] and it has been recently demonstrated that inclusion of crystal field effects into theoretical INDO/S studies of the spectra of both adenine and guanine can lead to significant changes of calculated transition moment directions, relative to those of the isolated molecules.[63,64] Moreover, Stewart and Davidson[60] noted that there is a red shift and large intensity reduction of band I of 9-methyladenine crystals relative to the spectrum in solution. The intensity changes were judged greater than would be expected from exciton interactions, and are a clear demonstration that band I is easily perturbed by the external environment. The differences in the polarized reflectance spectra of band I in 9-methyladenine and 6-(methylamino)purine reported by Clark[61] tend to support this idea as well. In the following analysis, we consider in more detail the factors which

(63) Theiste, D.; Callis, P. R.; Woody, R. W. *Biophys. J.* **1990**, *57*, 455a.
(64) Sreerama, N.; Woody, R. W.; Callis, P. R. *Biophys. J.* **1990**, *57*, 455a.

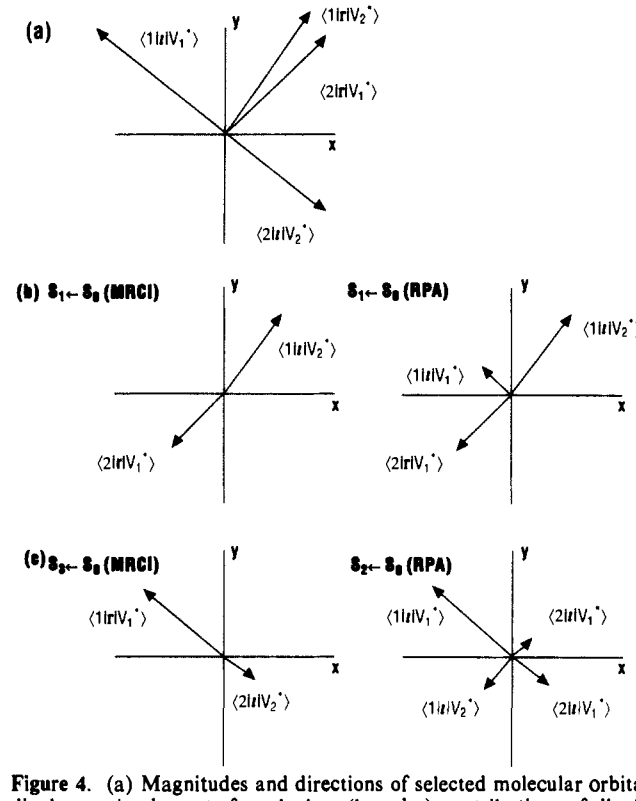

Figure 4. (a) Magnitudes and directions of selected molecular orbital dipole matrix elements for adenine; (b and c) contributions of dipole matrix elements to the transition dipoles (eq 7 and 11) of selected transitions of adenine.

can lead to uncertainties in the polarization of band I.

Among the singly excited configurations listed in Table V, the four which provide matrix elements $\langle \varphi_i | \mathbf{r} | \varphi_a \rangle$ that give large contributions to the transition dipole are the valence $\pi \rightarrow \pi^*$ excitations $\Phi(1 \rightarrow V_1^*)$, $\Phi(2 \rightarrow V_1^*)$, $\Phi(1 \rightarrow V_2^*)$, and $\Phi(2 \rightarrow V_2^*)$, where the orbitals are listed in Table I. The remaining configurations contribute matrix elements with much smaller values and may be neglected in the present analysis. Figure 4a shows a vector representation of each matrix element in the xy plane; all have about the same magnitude and two pair are polarized mutually perpendicular, with $\theta = +45°$ or $\theta = -45°$.

Figure 4b shows the four matrix elements, weighted by the appropriate coefficients $C_{00}C_K(i \rightarrow a)$ (MRCI) or $\{X_{ia,K} + Y_{ia,K}\}$ (RPA) (see Table V), as they contribute to the $S_1 \leftarrow S_0$ transition dipole. In the MRCI calculation, the resultant transition dipole comes from a near cancellation of two large colinear vectors, $\langle 1|\mathbf{r}|V_2^* \rangle$ and $\langle 2|\mathbf{r}|V_1^* \rangle$. Analysis of the RPA results shows different behavior, in which vectors $\langle 1|\mathbf{r}|V_2^* \rangle$ and $\langle 2|\mathbf{r}|V_1^* \rangle$ cancel, but the presense of a small contribution from $\langle 1|\mathbf{r}|V_1^* \rangle$ determines the polarization of the transition while still giving a relatively small oscillator strength.

The analysis of the intense band I transition is shown in Figure 4c. In the MRCI calculation only two vectors contribute strongly, and there is a partial cancellation between $\langle 1|\mathbf{r}|V_1^* \rangle$ and $\langle 2|\mathbf{r}|V_2^* \rangle$ to yield a resultant transition dipole whose polarization is approximately $\theta = +40°$ to $\theta = +50°$. In the RPA calculation there is also a partial cancellation between $\langle 1|\mathbf{r}|V_1^* \rangle$ and $\langle 2|\mathbf{r}|V_2^* \rangle$ as well as a cancellation between significant contributions from $\langle 1|\mathbf{r}|V_2^* \rangle$ and $\langle 2|\mathbf{r}|V_1^* \rangle$, but the resultant polarization is similar to the MRCI result.

Considering the above analysis, band I is seen to contain a pair of nearly degenerate transitions whose intensities are derived from a weighted sum of four vector components. The intensity magnitudes are determined by the extent of certain cancellations. Furthermore, both the magnitude and direction of the transition dipoles are clearly sensitive to excited-state composition, as shown by the differences between the present MRCI and RPA results. From a theoretical viewpoint, an environmental perturbation would be reflected in changes in molecular orbitals and their energies,

which in turn would alter the mixing of the two degenerate states and/or the mixing of the principal single excitations within each excited state. Given the complex composition of the transition dipoles in the two degenerate excited states, even minor perturbations could likely have significant effects on the intensity and polarization of band I.

Guanine: Bands I and II. The low-energy spectral region of guanine shown in Figure 3 contains a broad band with two maxima at 36 300 cm^{-1} (275 nm, band I) and 40 000 cm^{-1} (250 nm, band II). Callis et al.[65] and Clark[66] have investigated the spectrum of single crystals of 9-ethylguanine using reflectance techniques which unequivocally establish the polarization of band II to be $\theta = -75°$. The polarization of band I is generally accepted as being $\theta = -4°$ from crystal and linear dichroism studies.[6,59,66] A variety of semiempirical studies of the guanine spectrum have been reported,[13-15,17,20,21] and generally they assign single valence $\pi \rightarrow \pi^*$ transitions to bands I and II. The calculated polarizations from these studies are reasonably consistent, giving values of $\theta = -60°$ to $\theta = -70°$ and $\theta = +30°$ to $\theta = +45°$ for bands I and II, respectively, which do not agree with the experimental values.

The resolution of the low-energy spectral region of guanine obtained from the present MRCI and RPA calculations shown in Figure 3 reveals the presence of no fewer than six transitions: two $\pi \rightarrow \pi^*$ transitions in band I; one $\sigma \rightarrow \pi^*$ and three $\pi \rightarrow \pi^*$ transitions in band II. The data for the five low-energy $\pi \rightarrow \pi^*$ transitions of guanine given in Table V show that each transition contains a mixture of Rydberg and valence excitations. Thus, both the number and characteristics of the transitions in this spectral region found in the current studies differ markedly from those obtained from semiempirical methods.

An analysis of the contributions of the principal single excitations (Table V) to the transition dipoles (eq 7 and 11) shows that only the two valence excitations $\Phi(1\rightarrow V_1^*)$ and $\Phi(1\rightarrow V_2^*)$ contribute strongly to the intensity of each transition. The relevant matrix elements $\langle 1|r|V_1^*\rangle$ and $\langle 1|r|V_2^*\rangle$ each have a magnitude of approximately 1.35 au and are polarized nearly perpendicular, with $\theta = -25°$ and $\theta = +70°$, respectively. However, the presence of two degenerate transitions within band I and three degenerate $\pi \rightarrow \pi^*$ transitions in band II means that mixing of states due to environmental perturbations is probably more severe than in the lowest band in adenine. Furthermore, from a computational viewpoint, it is expected that both the mixing of degenerate transitions and the proportions of valence and Rydberg excitations in the transitions which contribute to bands I and II will vary somewhat with the level of calculation, which in turn may significantly alter the calculated polarizations. This is demonstrated in the present study by the data in Table V, which show differences in the composition of the three nearly degenerate transitions of band II obtained in the MRCI calculations ($S_3 \leftarrow S_0$, $S_5 \leftarrow S_0$, and $S_6 \leftarrow S_0$), compared with those from the RPA studies ($S_3 \leftarrow S_0$, $S_4 \leftarrow S_0$, and $S_6 \leftarrow S_0$). Thus, we conclude that the low-energy spectral region in guanine is inherently too complex to permit the calculation of individual transition polarizations, which themselves are likely to vary considerably with both the level of theory and the molecular environment.

Higher Lying Transitions. In the spectral region of both molecules from 45 000 to 55 000 cm^{-1}, there are a large number of closely spaced transitions of varying intensity. The transitions which provide the intensity are all of the $\pi \rightarrow \pi^*$ type and are easily identified (see Figures 2 and 3). In general, however, there are no apparent correlations between either the number or composition of the transitions obtained with the MRCI and RPA calculations, respectively. For instance, in adenine the absorption maximum at approximately 47 500 cm^{-1} is predicted to arise in the MRCI calculations from the ($S_{10} \leftarrow S_0$), ($S_{12} \leftarrow S_0$), and ($S_{13} \leftarrow S_0$) transitions, or in the RPA studies from the ($S_9 \leftarrow S_0$) and perhaps the ($S_6 \leftarrow S_0$) and ($S_7 \leftarrow S_0$) transitions. Hence, the two methods provide different details of the resolution of this spectral region, which is not surprising since with excessive spectral congestion different mixings within groups of nearly degenerate states are likely to occur. Therefore, although both the MRCI and RPA results account for the qualitative features of this spectral region, a more detailed analysis beyond the general picture provided by Figures 2 and 3 does not appear to be appropriate in the current study.

Table VI. Mulliken Net Atomic Charges of the SCF Ground State

adenine		guanine	
N_1	−0.325	N_1	−0.651
C_2	−0.098	C_2	0.552
N_3	−0.212	N_3	−0.278
C_4	0.296	C_4	0.313
C_5	0.084	C_5	0.012
C_6	0.401	C_6	0.450
N_7	−0.267	N_7	−0.181
C_8	−0.050	C_8	−0.095
N_9	−0.558	N_9	−0.563
H_{10}	0.210	H_{10}	0.210
H_{11}	0.387	H_{11}	0.379
H_{12}	0.196	O_{12}	−0.444
N_{13}	−0.804	H_{13}	0.381
H_{14}	0.369	N_{14}	−0.812
H_{15}	0.373	H_{15}	0.342
		H_{16}	0.386

Triplet States. Considering the triplet-state data in Table III, MRCI calculations on adenine predict that there are no fewer than four triplet (π,π^*) states positioned at lower energies than the lowest singlet state. The lowest triplet state T_1 is estimated to be only 24 930 cm^{-1} above the ground state, based on the same linear scaling of calculated triplet transition energies used for singlet transitions.[50] The values of $\langle z^2\rangle$ of the charge distributions of the lowest seven triplet states appear to be similar to the ground state, while some of the higher triplet states do exhibit some Rydberg character. In guanine there are a pair of closely spaced low-lying valence triplet (π,π^*) states estimated to be 28 280 and 29 520 cm^{-1} above the ground state, while the next triplet (π,π^*) states, T_3 and T_4, are predicted to be isoenergetic with the singlet states within band I. The present energy estimates for T_1 appear to be reasonable, since the low-temperature phosphorescence spectra of adenosine and guanosine[67] both have broad maxima at 23 000–25 000 cm^{-1}. Moreover, semiempirical triplet-state calculations[9,12,18] place T_1 within a range of 20 000–30 000 cm^{-1}.

Ground-State Properties

In addition to the present calculations on excited states, a number of ground-state properties were also obtained and are briefly summarized here. The SCF total energies of adenine and guanine are −466.454 57 and −539.302 67 hartrees, respectively. The SCF ground-state charge distributions given in terms of Mulliken net atomic charges[68] are present in Table VI. Singh and Kollman[27] have also reported net atomic charges for adenine and guanine, determined from least-squares fits of quantum mechanical electrostatic potentials calculated with minimum basis sets. Generally, there is little agreement between the present charges and those of Singh and Kollman, particularly on the nitrogen atoms with lone pairs (N_1, N_3, and N_7, adenine; N_3 and N_7, guanine), where Singh and Kollman predict a much higher electron density than calculated in the present study.

The ground-state total energies from MRCI wave functions for adenine and guanine are −466.495 78 and −539.334 71 hartrees, respectively. The ground-state molecular dipole moments computed from MRCI wave functions are 2.68 D ($\theta = -84°$) and 7.89 D ($\theta = +158°$) for adenine and guanine, respectively, where the angle θ defined in Figure 1 specifies the orientation of the dipole vector (defined as pointing negative to positive). The experimentally determined dipole moment of 9-butyladenine is 3.0 ± 0.2 D.[69] The experimental dipole moment value of guanine is

(65) Callis, P. R.; Fanconi, B.; Simpson, W. T. *J. Am. Chem. Soc.* **1971**, *93*, 6679–6680.
(66) Clark, L. B. *J. Am. Chem. Soc.* **1977**, *99*, 3934–3938.
(67) Bersohn, R.; Isenberg, I. *Biochem. Biophys. Res. Commun.* **1963**, *13*, 205–208.
(68) Mulliken, R. S. *J. Chem. Phys.* **1955**, *23*, 1833–1840.

not available, but the present level of theory is expected to provide a good approximation.

Summary and Conclusions

In the present ab initio studies of adenine and guanine, both the MRCI and RPA calculations have revealed the presence of 20 to 25 singlet-singlet electronic transitions in the spectral region between 35 000 and 55 000 cm^{-1}, a number considerably higher than is predicted by semiempirical calculations. Errors in calculated transition energies obtained with both the MRCI and RPA methods were found on average to fall within a range of 12 000-15 000 cm^{-1}, and linear scalings of calculated transition energies have been used to provide an approximate qualitative resolution of the absorption spectra.

The lowest absorption band of adenine at 38 500 cm^{-1} (band I) is shown by both methods to arise from a group of two $\sigma \rightarrow \pi^*$ and three $\pi \rightarrow \pi^*$ electronic transitions, only one of which is calculated as intense. In guanine, band I at 36 300 cm^{-1} contains two $\pi \rightarrow \pi^*$ transitions, and band II at 40 000 cm^{-1} arises from one $\sigma \rightarrow \pi^*$ and three $\pi \rightarrow \pi^*$ transitions. The calculated polarizations of these bands do not agree with experimental values obtained for crystals. It is clear, however, that the actual polarizations are likely to be very sensitive to changes in molecular environment, and that calculated polarizations are quite sensitive to the level of theory. Therefore, it appears that it is not possible to obtain or assign definite values for the polarizations of the low-energy bands.

In the spectra of both molecules between 45 000 and 55 000 cm^{-1}, a large number of transitions of varying intensity were found in both the MRCI and RPA studies, but the number and characteristics of the constituent transitions found differ between the two methods. Nevertheless, the general features of the broad-banded absorption in this spectral region are described by both methods.

Adenine and guanine each possess several triplet (π,π^*) states which lie lower in energy than the lowest excited singlet state, S_1. In adenine, there are four triplet (π,π^*) states below the lowest excited singlet state, with T_1 predicted to lie only 24 930 cm^{-1} above the ground state, S_0. In guanine, T_1 and T_2 are located at approximately 28 280 and 29 520 cm^{-1} above S_0, respectively, with T_3 and T_4 isoenergetic with S_1.

Thus, it appears that the current ab initio investigation of the spectral properties of adenine and guanine has uncovered a number of subtle features heretofore unrecognized in earlier theoretical studies. Specifically, use of a more extended basis set which includes diffuse functions has, not unexpectedly, given rise to a considerably denser manifold of excited states. And as was shown, the resultant near degeneracy of several transitions in each of the spectral regions of interest leads to an enhanced sensitivity of the calculated polarizations to the level of theory employed. An important consequence of this is that the results of high-level calculations such as those described here may not be sufficient to produce reliable transition density distributions for use in exciton calculations. Furthermore, the spectral congestion revealed in the present study strongly suggests that experimentally determined polarizations of transitions determined for crystals are not expected to be valid in other molecular environments. Thus, both adenine and guanine possess absorption spectra which lack simplicitly, in that there are no bands in which the intensity is provided by a single isolated transition, which could be more easily characterized both theoretically and experimentally.

(69) DeVoe, H.; Tinoco, I. *J. Mol. Biol.* **1962**, *4*, 500-517.

Computational Studies of Open-Shell Phosphorus Oxyacids. 1. P-H Bond Homolysis in H_2PO_2

Christopher J. Cramer* and George R. Famini

Contribution from the U.S. Army Chemical Research Development and Engineering Center, Research Directorate, Physics Division, Chemometric and Biometric Modeling Branch, Aberdeen Proving Ground, Maryland 21010-5423. *Received February 5, 1990*

Abstract: The hypothetical molecule dihydrodioxophosphoranyl (**1**) has been studied computationally. Both 3-21G(*) and 6-31G* unrestricted Hartree-Fock (UHF) wave functions exhibited inherent doublet instability which was corrected for by consideration of correlation effects. Configuration interaction proved most effective in this respect, while Møller-Plesset perturbational corrections were fair when extended to third order and only marginal when truncated at second order. The barrier to P-H bond homolysis was determined to be 4.8 ± 0.3 kcal/mol. The metastability of **1** has been explained in the formalism of valence bond theory. It arises from interactions of degenerate valence bond functions corresponding to reactants and products with an intermediate configuration corresponding to a $n \rightarrow \pi^*$ ($^1A_2 \rightarrow {}^3B_1$) excited state. Predicted spectral data to aid in the identification of **1** are presented.

Organophosphorus compounds are ubiquitous in nature. Indeed, organophosphate intermediates are involved in nearly all energy transformations in living matter.[1] In the environment, organophosphorus species may be found in many forms, including fertilizers, detergents, and pesticides. The latter class can pose particular environmental problems with respect to long-term contamination.[2] This is especially the case when a compound exhibits significant mammalian neurotoxicity as an acetylcholine esterase inhibitor,[3] and the development of effective detoxification procedures for these compounds has occupied numerous research groups for many years.[4]

A large number of neurotoxic pesticides are organophosphonates, i.e., phosphorus(V) species with a single phosphorus-carbon bond. It has been observed that the microorganism

(1) Classical references include: (a) Erecinska, M.; Wilson, D. F. *Trends Biochem. Sci.* **1978**, *3*, 219. (b) Newsholme, E. A.; Start, C. *Regulation in Metabolism*; Wiley: New York, 1973. (c) Kelcker, H. M. *Biological Phosphorylations*; Prentice-Hall: New York, 1969.

(2) (a) Becker, E. L.; Fukoto, T. R.; Boone, B. Canham, D. C.; Boger, E. *Biochemistry* **1963**, *2*, 72. (b) *Organophosphorus Pesticides: Organic and Biological Chemistry*; Eto, M., Ed.; CRC Press: Cleveland, 1974.

(3) Main, R. A.; Iverson, F. *Biochem. J.* **1966**, *100*, 525.

(4) (a) Biresaw, G.; Bunton, C. A.; Quan, C.; Yang, Z.-Y. *J. Am. Chem. Soc.* **1984**, *106*, 7178. (b) Bunton, C. A.; Mhala, M. M.; Moffatt, J. R.; Monarres, D.; Savelli, G. *J. Org. Chem.* **1984**, *49*, 426. (c) Moss, R. A.; Swarup, S. *Tetrahedron Lett.* **1984**, 4079. (d) Rutkovskii, G. V.; Begunov, A. V.; Kuznetsov, S. G. *J. Org. Chem. USSR* **1983**, *19*, 701. (e) Rutkovskii, G. V.; Begunov, A. V.; Ignat'ev, Y. A. *Ibid.* **1983**, *19*, 710. (f) Bunton, C. A.; Gan, L.-H.; Savelli, G. *J. Phys. Chem.* **1983**, *87*, 5491. (g) Emsley, J.; Hall, D. *The Chemistry of Phosphorus*; Wiley: New York, 1976; pp 494-509. (h) Fendler, J. H.; Fendler, E. J. *Catalysis in Micellar and Micromolecular Systems*; Academic Press: New York, 1975; pp 150-161.